Geomechanics and Engineering, *Vol. 41, No. 1 (2025) 93-101*
https://doi.org/10.12989/gae.2025.41.1.093

Localized compressive strength profiling of sand MICP-treated by surface percolation method in 1D column

Turab Haider Jafri[a] and Jinung Do*

Department of Ocean Civil Engineering, Gyeongsang National University, Tongyeong, Republic of Korea

(*Received November 18, 2024, Revised March 5, 2025, Accepted March 10, 2025*)

Abstract. Biocementation in soils using microbially induced calcium carbonate precipitation (MICP) has recently emerged as a sustainable and environmentally friendly solution for improving the geotechnical characteristics of soils. The improvement level of MICP-treated sands varies depending upon the transportation and cementation mechanisms related to the methods of MICP implementation. Despite the conventional methods of strength measurement being used widely for MICP-treated soils, the influence of biocementation in soils resulting in a localized strength pattern has not been investigated yet. In this study, the localized strength profiling in unsaturated sand treated by MICP is carried out using a number of sand column tests under different treatment conditions. The MICP treatment was conducted using sand columns 10 cm in height and 5 cm in diameter through a surface percolation method. Unconfined compressive strengths (UCSs) along the depth of MICP-treated sand columns were measured in the form of local compressive strength through a needle penetration testing performed throughout the equally divided sections along the depth of the sand columns. The local water content and the local $CaCO_3$ content in each section were also quantified to investigate the dependence of local compressive strength on these factors. Moreover, the microscale examination of the specimens from MICP-treated sand columns was also performed. The investigation of local compressive strength measurement in MICP-treated sand columns in this study leads to deeper understanding of the factors affecting the local compressive strength. This work is expected to be a useful contribution to optimizing the practical application of MICP technology for green infrastructure development.

Keywords: biocementation; local compressive strength; MICP; needle penetration test; sand column; surface percolation

1. Introduction

Biocementation is an emerging soil stabilization approach that improves soil strength and stiffness by binding particles through microbial processes, offering a more sustainable solution than conventional chemical stabilization (DeJong *et al.* 2010). Among the various biocementation approaches, microbially induced calcium carbonate precipitation (MICP) is one of the most effective methods (Choi *et al*. 2020). In this method, microbial activity induces the precipitation of calcium carbonate ($CaCO_3$), which acts as a natural cement, increasing the load-bearing capacity and reducing soil settlement. This process is particularly effective in coarse-grained soils such as sand, where calcite cementation forms particle bridges at grain contacts (Li *et al*. 2023, Wang *et al*. 2023). Biocementation techniques not only enhance geotechnical properties, but also have the advantage of being environmentally friendly compared to conventional synthetic cement-based methods, which contribute significantly to carbon emission reduction (Ashraf *et al.* 2017, Cheng *et al.* 2014, Cheng and Shahin 2019, Fouladi *et al*. 2024, Ivanov *et al.* 2019, Kalkan 2020, Nawarathna *et al.* 2022, Pratama *et al*. 2024, Sierra *et al*. 2024, Wang *et al.* 2022).

MICP uses bacteria that break down urea ($CO(NH_2)_2$) into ammonium (NH_4^+) and carbonate ions (HCO_3^-). These carbonate ions then combine with calcium (Ca^{2+}) to form calcium carbonate ($CaCO_3$), which acts like a natural cement within the soil system (Eq. (1)). MICP has been used in various geotechnical applications, including controlling liquefaction (O'Donnell *et al*. 2017) and erosion (Do *et al.* 2019), slope stabilization (Gowthaman *et al*. 2019), and soil strengthening beneath foundations (DeJong *et al.* 2010).

$$CO(NH_2)_2 + H_2O \rightarrow 2NH_3 + CO_2 \quad (1a)$$

$$2NH_3 + 2H_2O \rightarrow 2NH^+{}_4 + 2OH^- \quad (1b)$$

$$CO_2 + OH^- \rightarrow HCO_3{}^- \quad (1c)$$

$$Ca^{2+} + HCO_3{}^- + OH^- \rightarrow CaCO_3 + H_2O \quad (1d)$$

In general, two primary techniques are used to implement MICP: injection and surface percolation methods. In the injection approach, bacterial and cementation solutions are directly injected into the soil at predefined depths, targeting specific layers for treatment. This method offers the advantage of targeting specific soil layers, but its effectiveness is limited because it often causes a significant reduction in permeability near the injection zone, resulting in the clogging of surrounding soils (Shahrokhi-Shahraki *et al.* 2015, Maleki Kakelar *et al.*

*Corresponding author, Associate Professor
E-mail: jinung@gnu.ac.kr
[a]Ph.D., Postdoctoral Researcher

ISSN: 2005-307X (Print), 2092-6219 (Online)

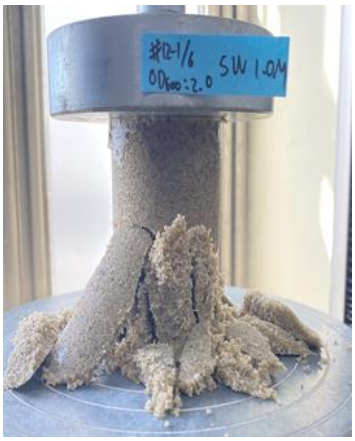

Fig. 1 Failure mode of sand treated by the MICP surface percolation method during UCS testing. The lower part crumbles first because there is less cementation than in the upper part.

2020, Konstantinou *et al*. 2021). In contrast, in the surface percolation method, bacteria and cementation solutions are sprayed onto the soil surface, allowing the solution to infiltrate the ground via gravitational drainage. The surface percolation method is particularly effective for treating soil surfaces rather than deeper depths (Cheng and Cord-Ruwisch 2014). Although the surface percolation method facilitates the treatment of the soil surface, challenges such as preferential flow paths and non-uniform distribution of $CaCO_3$ can result in heterogeneous soil properties.

Among the different soil properties, unconfined compressive strength (UCS) of soil is commonly used to evaluate the strength of biocemented soils (Lv *et al*. 2021, Mahawish *et al.* 2019, Wang and Yin 2021, Xiao *et al*. 2019). In unsaturated conditions, the MICP solution percolates into the soil owing to gravity, and the MICP reaction occurs according to the solution transfer characteristics. This results in heavy cementation near the soil surface, whereas the deeper soil remains less cemented. Conventional UCS testing of such samples often leads to crumbling of the lower part of the samples before reaching peak strength, as shown in Fig. 1. Furthermore, the compressive strength of MICP-treated soil has been observed to be varying locally along the soil with respect to the point of introduction of MICP-solution to the soil (Cheng and Cord-Ruwisch 2012). This observation emphasizes the need to analyze the compressive strength of MICP-treated soil samples at a local level.

To optimize the performance of the MICP surface percolation method, it is important to understand how the local compressive strength develops within the soil system. Therefore, the concept of measuring the local compressive strength of MICP-treated sand was introduced in this study using an experimental approach and microscale analysis. Several cylindrical column apparatuses were prepared with unsaturated sand and then treated with the MICP solution for strength enhancement. The local UCS, water content, and mass of $CaCO_3$ were measured along the depth of the sand columns after completing the MICP treatment, and the dependence of the local UCS on the local water content and mass of $CaCO_3$ was analyzed under different testing conditions. Furthermore, scanning electron microscopy (SEM) analysis of samples taken from the treated sand columns was performed to investigate the microscale changes owing to MICP treatment and relate them to the change in local compressive strength. Profiling the compressive strength along the depth provided insight into the mechanism of MICP implementation using the surface percolation method.

Table 1 Geotechnical properties of Jumunjin sand used in this study

Specific gravity, G_s	2.61
Maximum void ratio, e_{max}	0.96
Minimum void ratio, e_{min}	0.58
Relative density, D_γ [%]	85.3
Initial void ratio, e	0.636
Mean grain size, D_{50} [mm]	0.57

2. Methodology

2.1 Preparation of MICP solution

The MICP solution used in this experimental study was prepared by mixing a biological solution and a cementation solution. The urease-producing bacterial strain used in this study was *Sporosarcina pasteurii* (KACC 11249, available from the Korean Agricultural Culture Collection). The biological solution was prepared by incubating the bacterial strain in a 1-liter solution of growth media, which consisted of 20 g/L yeast extract, tris-buffer 15.79 g/L, and 10 g/L ammonium sulfate. The incubation of the bacterial strain in the growth media was performed in a shaking incubator at 200 rpm and 30°C. The maximum incubation level of the biological solution was established at an optical density at 600 nm wave length (OD_{600}) of 1.8 and the incubation process took around 40 hours to complete. The biological solution was then centrifuged at 4,000 rpm for 15 min and stored at 4°C before being used to prepare the MICP solution. The cementation solution was prepared at different concentration levels, which consisted of respective molarities of urea ($CO(NH_2)_2$) and calcium chloride dihydrate ($CaCl_2.2H_2O$). The concentrations of the solutions used in this study were 0.1, 0.3, 0.5, 0.7, and 1.0 M.

2.2 Preparation of sand columns

The soil used in this study was Jumunjin sand and its geotechnical properties were used to calculate the pore volume of the test specimens (Table 1). The test apparatus consisted of a rigid acrylic column with a perforated base to allow drainage of the MICP solution percolating through the soil, as shown in Fig. 2(a).

Columns with a total height of 13 cm and inner diameter of 5 cm were filled with sand up to a height of 10 cm. Using

(a) Soil column filled with sand

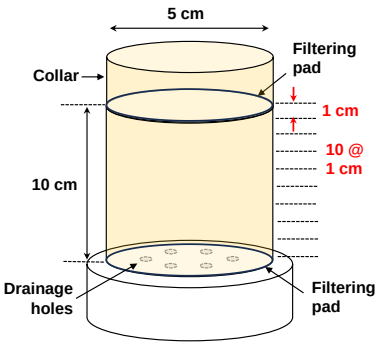

(b) Schematic of the sand column testing setup

Fig. 2 Composition of the sand column apparatus

the dimensions of the cylindrical sand specimen held within the column and the sand properties, the pore volume was calculated to be approximately 75 cm^3. Filtering pads were placed at the top and bottom of the sand specimens to allow uniform spraying of the MICP solution and avoid scouring the sand surface. A schematic diagram of the test apparatus is shown in Fig. 2(b).

2.3 MICP treatment

To induce sufficient $CaCO_3$ cementation in the soil, the MICP solution was used to fill two pore volumes of the sand column. The ratio of the biological and cementation solution was maintained at 1:5 throughout the experiment. Thus, the quantities of the biological and cementation solutions to be used in each treatment were calculated as 30 and 150 ml, respectively, according to the two pore volumes of the MICP solution selected for introduction to the soil columns used in this study. Both the biological and cementation solutions were transferred to the soil simultaneously so that the MICP reaction took place within the soil medium. All sand columns were treated with the MICP solution five times at 24 h intervals between treatments. The MICP reaction was halted 24 h after the last treatment by flushing the soil medium with water equal to the two pore volumes in the sand column. This treatment procedure was used for all sand columns prepared for this study.

2.4 Measurement of local compressive strength, water content, and mass of $CaCO_3$

After completion of the MICP treatment, the local compressive strength, water content, and mass of $CaCO_3$ were evaluated at each 1 cm section along a 10 cm depth of the treated specimen. Local compressive strength measurements were conducted using a needle penetrometer as shown in Fig. 3(a) (SH-70, Maruto Corporation, Japan). The test procedure involved penetrating a needle up to 10 mm into the treated surface and recording the Needle Penetrometer Index (*NPI*), which was used to indirectly calculate the strength. A needle penetrometer can be used for forces up to 100 N, which can be recorded from the load scale. After the needle penetrated the soil surface, the penetration depth (D) and load value (F) were recorded, and the needle was slowly removed. In cases where F reached 100 N, the needle was withdrawn before reaching a penetration depth of 100 mm. The *NPI* values were calculated using (Eqs. 2(a) and 2(b)).

$$NPI = F/10 \text{ for } D = 10 \text{ mm and } F \leq 100 \text{ N} \quad (2a)$$

$$NPI = 100/D \text{ for } D \leq 10 \text{ mm and } F = 100 \text{ N} \quad (2b)$$

Three *NPI* readings were obtained at each section according to the testing pattern shown in Fig. 3(b). The average of the three *NPI* readings taken at each section was converted to UCS using (Eq. (3)).

$$UCS \text{ [MPa]} = \left(10^{0.98 \log NPI + 2.621}\right)/1000 \quad (3)$$

The process of determining the local compressive strength was initiated by recording *NPI* values at the surface of the treated specimen, followed by careful excavation of the top 1 cm section with a spatula so that the soil located in the next section remained undisturbed. When the surface of the next section was visible after disintegrating the first section, *NPI* readings were taken again, and the process continued to the last section at the bottom of the treated specimen. Thus, ten averaged *NPI* readings were recorded along the column depth, which were converted to local compressive strength.

Disintegrated specimens collected from each section were used to calculate the water content and mass of $CaCO_3$. The specimens were dried and acid-washed using 1N HCl, and the weight of the dry soil and $CaCO_3$ content were measured separately. The percentage ratio of $CaCO_3$ content and weight of dry soil after acid washing was termed the local mass of CaCO3, m_c in this study, and the percentage ratio of the weights of oven-dried specimens before and after acid washing was used as the local water content, w.

All experiments were performed at a temperature of 18°C. This test procedure was repeated to evaluate the local compressive strength w, and m_c along the column depth in all the sets of experiments conducted in this study.

3. Results and discussion

3.1 Effect of MICP treatment on local compressive strength, water content, and $CaCO_3$ content

In the first phase of the experiments, five sand columns were prepared and treated with MICP solutions at concentrations of 0.1, 0.3, 0.5, 0.7, and 1.0 M. The MICP reaction was terminated 24 h after the final treatment by percolating two volumes of water through the treated specimens. After 40 d, the specimens were tested for local compressive strength and w and m_c measurements. The effect of MICP treatment on the local compressive strength along the column depth is shown in Fig. 4. The concentration of the MICP solution significantly affected the overall strength of the treated columns. The strength increased with increasing concentration of the MICP

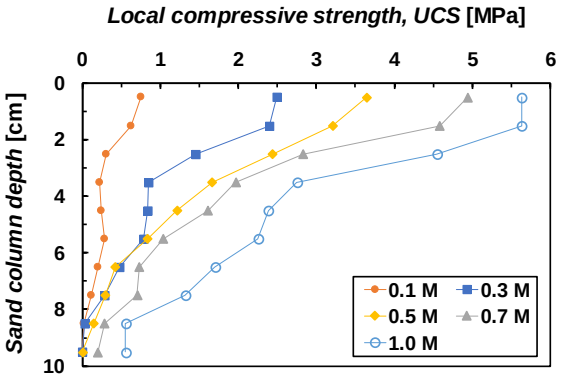

Fig. 4 Change in local compressive strength along the column depth with respect to the concentration of the MICP solution

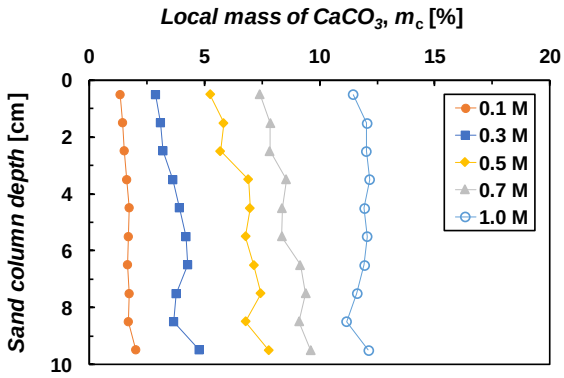

Fig. 6 Change in m_c along the column depth with respect to the concentration of the MICP solution

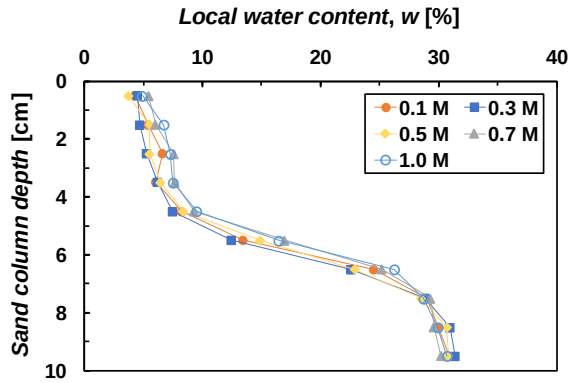

Fig. 5 Change in w along the column depth with respect to the concentration of the MICP solution

solution. The maximum local compressive strength was obtained in the upper sections of the treated columns, with the highest local compressive strength of 5.63 MPa in the top section of the sand column treated with 1.0 M MICP solution and the lowest local compressive strength of 0.76 MPa in that treated with 0.1 M solution. A clear pattern of local compressive strength gradually decreasing along the column depth after 40 d of MICP treatment was also observed. No significant strength improvement was observed in the lower part of the sand columns except for those treated with 0.7 M and 1.0 M MICP solutions. The minimum local compressive strength was obtained in the bottom section of all columns, with 0.55 MPa in the sand column treated with 1.0 M MICP solution and 0.01 MPa in that treated with 0.1 M solution.

The water content in each section along the column depth is expected to change with time due to surface evaporation and gravitational drainage phenomena. Therefore, it is important to record the variation in w at different intervals after the completion of treatments so that its potential effect on the localized strength could be analyzed. The effect of the MICP treatment on w along the column depth is shown in Fig. 5. The concentration of the MICP solution did not affect w because the same pattern along the depth was observed in all treated columns. An increase in w along the column depth was observed for all concentrations of the MICP solution.

The lowest w was obtained in the top section, with an average of 4.5%, and the highest was obtained in the bottom section, with an average of 30.8% w. w changed gradually up to 8% in the first five sections from the top 40 d after treatment, after which it changed significantly in the middle sections of the treated columns and remained constant at approximately 30% in the last three sections owing to the significant fluid accumulation in the bottom part of the sand columns.

The effect of the MICP treatment on m_c along the column depth is shown in Fig. 6. The concentration of the MICP solution controlled the overall accumulation of $CaCO_3$ in the treated specimens, because higher concentrations produced higher amounts of $CaCO_3$. The average m_c measured in each section along the column depth were 1.65%, 3.74%, 6.66%, 8.57%, and 11.85% in the respective sand columns treated with 0.1, 0.3, 0.5, 0.7, and 1.0 M concentrations of MICP solution. However, no significant change was observed in m_c along the column depth for any of the five treated sand columns. The standard deviations of m_c measured along the column depth were 0.18%, 0.55%, 0.77%, 0.69%, and 0.31% in the sand columns treated with all five concentrations of MICP solution used in this study. These results indicate that the decrease in local compressive strength along the sections of the MICP-treated sand column did not merely depend on m_c and remained almost unchanged along the column depth.

However, the change in local compressive strength depended on the variation in w along the column depth, as shown in Fig. 7. An overall declining trend in the local compressive strength related to w was observed 40 d after MICP treatment. Because m_c does not contribute to the changing local compressive strength along the column depth, further investigation of the change in local compressive strength in relation to the change in w with time during the 40 days after treatment was required, which is discussed in the next section. In addition, a sharp decrease in the local compressive strength was initially observed, although w did not vary significantly in the upper sections, as previously discussed. This indicates that other factors, apart from w, control the decrease in local compressive strength along the treated column depth. Hence, a microscale analysis of the samples obtained from the treated columns was performed to understand this phenomenon.

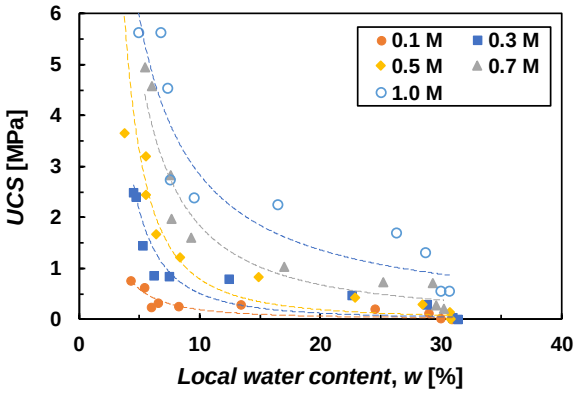

Fig. 7 Relationship between local compressive strength and w with respect to the concentration of the MICP solution

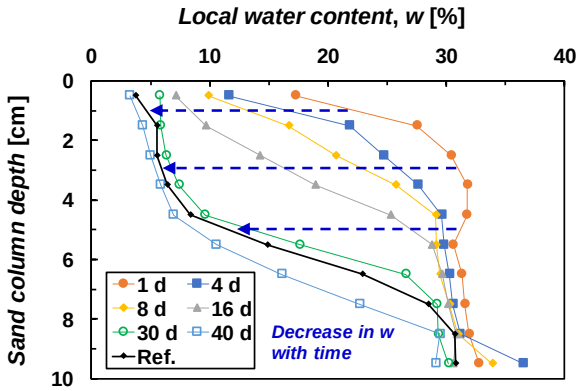

Fig. 9 Variation in w during the 40 d after MICP treatment

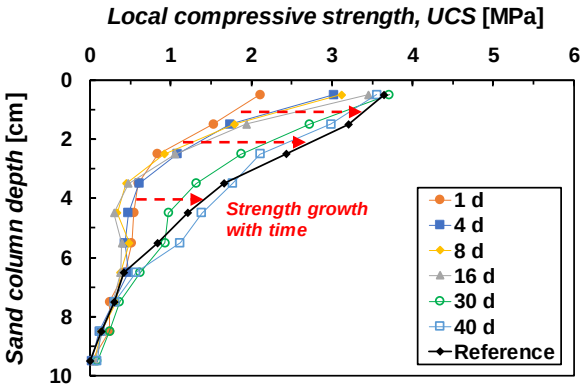

Fig. 8 Variation in local compressive strength during the 40 d after MICP treatment

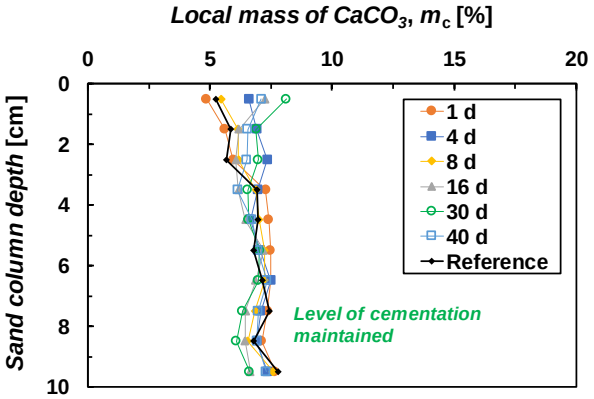

Fig. 10 Variation in m_c during the 40 d after MICP treatment

3.2 Incremental growth on local compressive strength and water content after MICP treatment

The conventional meaning of aging is a post-treatment effect that occurs after at least several months or years. However, there was a finding that UCS gradually increased during a limited time interval after the treatment (e.g., approximately 40 d). Thus, in the second phase of the experiments, the incremental change in the local compressive strength along with the change in w throughout the 40 d after treatment was investigated. The local compressive strength, w, and m_c were recorded at different time intervals over 40 d after MICP treatment. Hence, another set of experiments was conducted by treating six sand columns using the 0.5 M MICP recipe, followed by measurement of the local compressive strength, w, and m_c at 1, 4, 8, 16, 30, and 40 d after the treatment. The second phase of the experimental results needed to be analyzed with reference to the predetermined pattern of results obtained in the first phase. In this respect, the results obtained from the sand column treated with a 0.5 M concentration of MICP solution in the first phase experiments were set as a reference. The second-phase experimental results were analyzed in comparison with the reference so that the incremental changes in the local compressive strength and w could be understood in light of the first-phase experimental results.

The effect of MICP treatment with 0.5 M solution on the local compressive strength with respect to the column depth, recorded 40 d after treatment, is shown in Fig. 8. The local compressive strength along the column depth on Day 1 was significantly lower than that of the reference results, except at the bottom part of the column. The highest local compressive strength was 2.11 MPa measured at the top section of the treated column, which increased significantly to 3.02 MPa and 3.12 MPa, respectively, on Days 4 and 8, respectively. Apart from the first two sections at the top, the local compressive strength along the depth on Days 4 and 8 remained similar to that on Day 1. A further increase in the local compressive strength of the topmost section up to 3.45 MPa was observed on Day 16, but the remaining sections showed a similar trend of change in the local compressive strength as that on Days 4 and 8. The local compressive strength measured on Day 30 in the lower sections of the treated column was similar to the reference results. In contrast, the upper sections had slightly lower local compressive strength, except for the top section, which was identical to the reference results. On Day 40, the local compressive strength along all the sections was identical to the reference local compressive strength from the first phase of the experiment. These results indicate that the local compressive strength in most of the sections remained significantly low during the first 16 d after treatment. The first two sections from the top achieved considerable local compressive strength during the first 16 days, and major

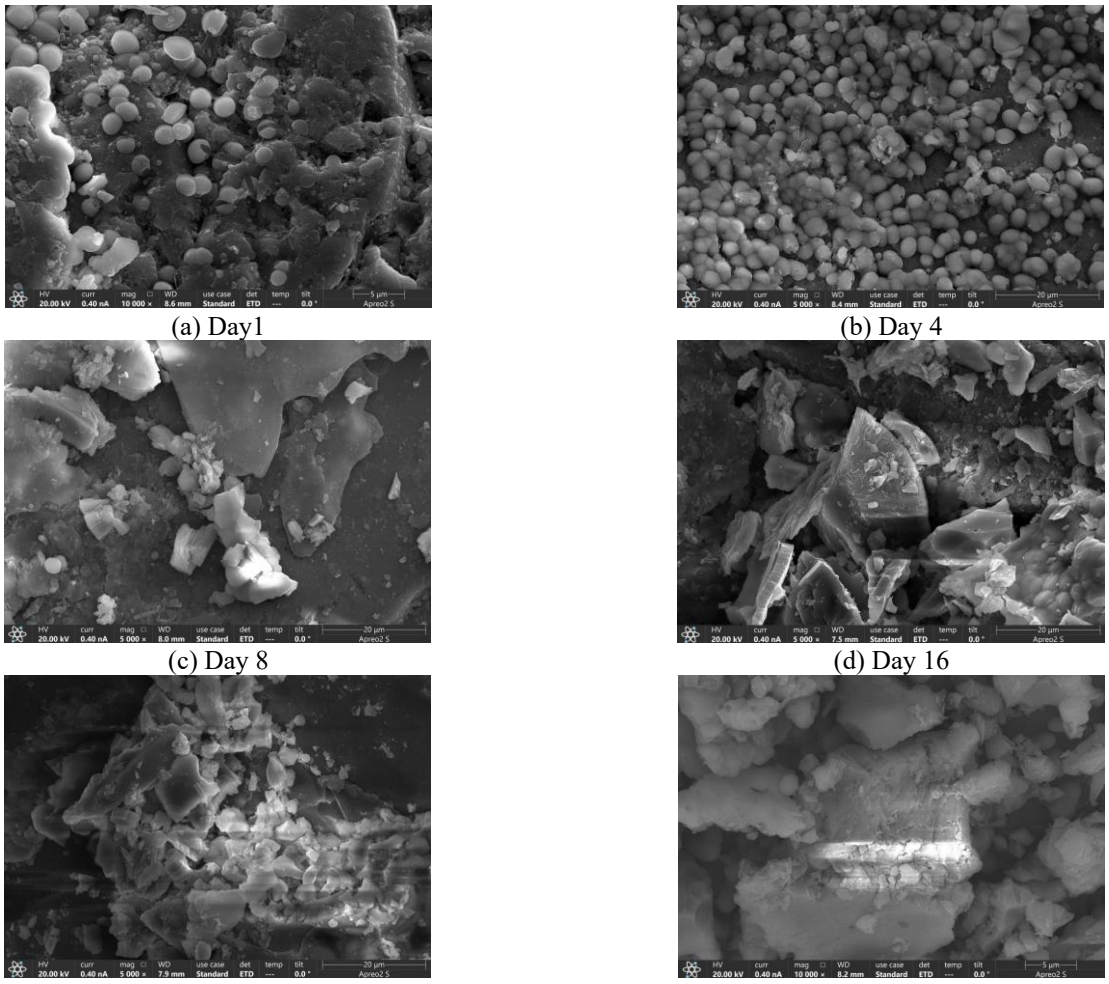

(a) Day1 (b) Day 4

(c) Day 8 (d) Day 16

(e) Day 30 (f) Day 40

Fig. 11 SEM analysis of specimens representing the upper section of MICP-treated sand columns during the 40 d after treatment

changes in the local compressive strength along the column depth required 16 to 30 d.

The effect of MICP treatment with 0.5 M solution on w and m_c with respect to column depth, recorded 40 d after treatment, are shown in Figs. 9 and 10, respectively. The m_c in all the treated columns showed trends similar to those in the first-phase experiments and did not change significantly along the column depth during the 40 d after treatment. The w value measured along the column depth on Day 1 was significantly higher than that of the reference results. The lowest w was observed in the top section, where it was measured as 17.29% on Day 1, and decreased significantly to 11.59% and 9.88% on Days 4 and 8, respectively. There was a homogeneous decrease in w in the upper half of the columns measured on Days 4 and 8; however, but the bottom half remained considerably high in w up to Day 16.

The lowest w on Day 16 was measured in the top section at 7.1%, and the rest of the sections showed a decreasing trend similar to that on Days 4 and 8. A significant decrease in w was observed along the column depth on Days 30 and 40 where w in all sections were almost identical to the reference results. The lowest w values on days 30 and 40 were measured in the top section, at 5.78% and 3.23%, respectively. These results show that a decrease in the local compressive strength occurs in parallel with an increase in w along the column depth, which confirms that w is a key factor in controlling the decrease in the local compressive strength along the column depth. The respective trends of variation in the local compressive strength and w measured 40 d after treatment were not completely identical, which led to the need for further investigation at the particle level.

3.3 Microscale analysis of MICP-treated sand

A microscale study of MICP-treated sand was required to observe the morphological changes in cemented $CaCO_3$ between sand particles. Thus, SEM analysis of the MICP-treated sand specimens was performed to gain a deeper understanding of the variation in the local compressive strength along the column depth. Soil specimens were collected from the sand columns treated with 0.5 M concentration of MICP solution in the second-phase experiments to allow analysis of the microscale variation during the 40 d after treatment. Representative specimens were collected from upper and lower sections of the treated

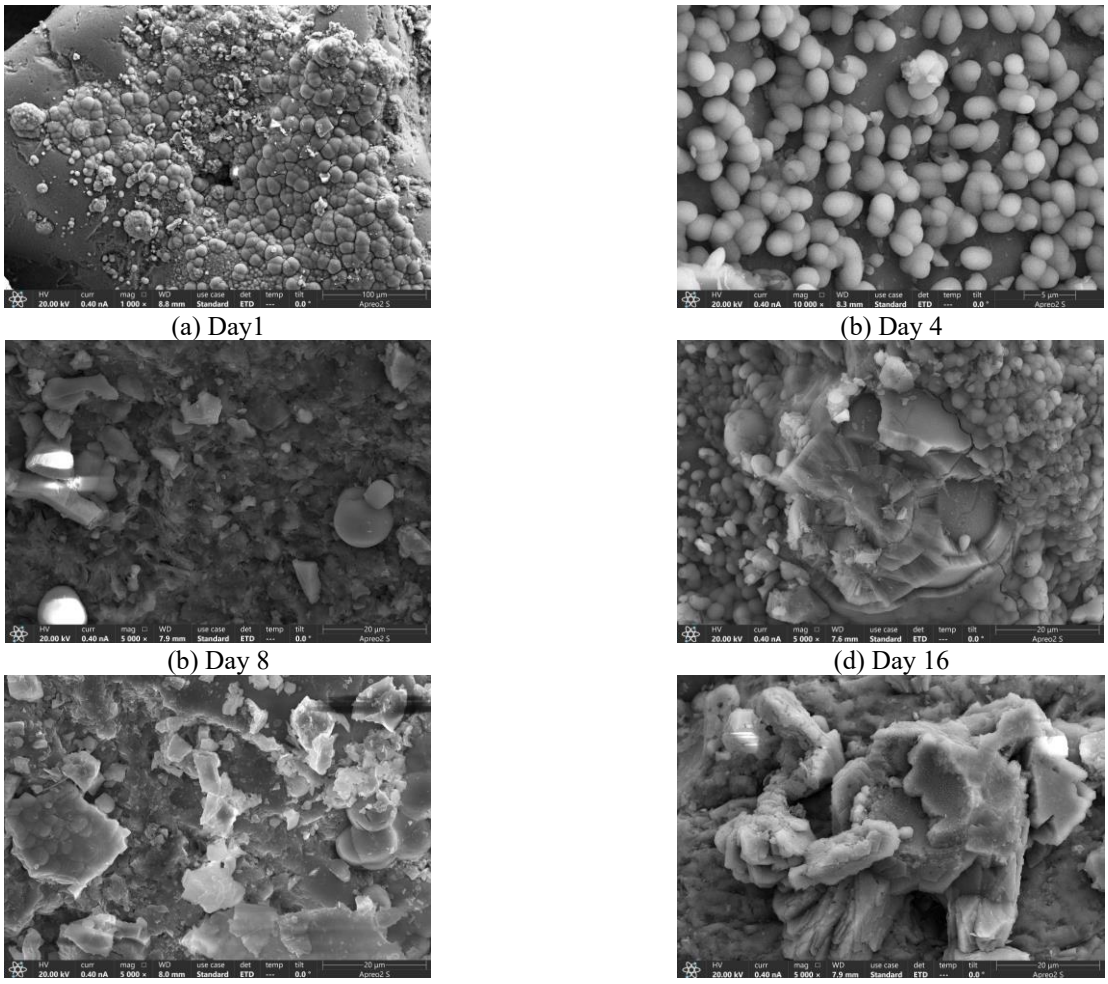

(a) Day1 (b) Day 4

(b) Day 8 (d) Day 16

(e) Day 30 (f) Day 40

Fig. 12 SEM analysis of specimens representing the lower section of MICP-treated sand columns during the 40 d after treatment

sand columns. One was collected from a section lying between 1 and 2 cm from the column surface, whereas the other was taken from a section lying between 6 and 7 cm.

SEM analyses of 12 samples collected from the treated specimens were conducted; six samples each represented the upper and lower sections. The SEM images of the specimens in the upper section of the MICP-treated sand columns on Days 1, 4, 8, 16, 30, and 40 are shown in Fig. 11. The morphology of the cemented $CaCO_3$ on Days 1 and 4 showed spherical in the upper section of the treated columns. The lower local compressive strength observed during the experimental phase on Days 1 and 4 is related to the unstable minerals with low bonding. A morphological change in the cemented $CaCO_3$ in the upper section was observed on Day 8, where the $CaCO_3$ minerals transformed into more stable $CaCO_3$ minerals in the treated specimen. The precipitated $CaCO_3$ in the cemented sand particles was continuously observed until Day 40. This trend, in combination with the decrease in w, explains the increase in the local compressive strength in the upper section of the MICP-treated sand columns.

SEM images of the specimens in the lower section of the MICP-treated sand columns on Days 1, 4, 8, 16, 30, and 40 are shown in Fig. 12. Similar to the upper section, the morphology of the cemented $CaCO_3$ on Days 1 and 4 showed spherical minerals in the lower section of the treated columns. Subsequently, the minerals began to transform into more stable form, and this morphological transformation of $CaCO_3$ in the lower section continued gradually until Day 40. Although $CaCO_3$ minerals were cemented between the sand particles, the presence of higher w restricted the increase in the local compressive strength in the lower section. These results led to the conclusion that the increase in the local compressive strength along the depth of the MICP-treated sand columns was due to the combined effects of changes in w and morphological changes in $CaCO_3$ cementation from vaterite to calcite minerals between the sand particles.

4. Conclusions

In this study, the effects of MICP treatment on the local compressive strength, w, and m_c measured in unsaturated sand were investigated. Several sand columns were treated with various concentrations of MICP solution using the

surface percolation method. The local compressive strength along the depth of the MICP-treated sand columns was measured via needle penetration tests. Moreover, the morphological changes in the MICP-treated sand specimens 40 d after treatment were also investigated. The main findings of this study are as follows.

a) The local compressive strength of the sand columns treated with MICP solution decreased along the column depth.
b) Treatment with a higher concentration of MICP solution resulted in a higher local compressive strength and vice versa, irrespective of the variation in the local compressive strength along the column depth.
c) m_c was unchanged significantly with the column depth. However, treatment with a higher concentration of the MICP solution resulted in a higher amount of $CaCO_3$ cementation between the sand particles.
d) The w is low in the upper section of the treated sand columns and high in the lower sections. The variation in w along the column depth occurred with respect to time.
e) The change in the local compressive strength along the depth of the MICP-treated sand columns depended on the change in w as well as the morphological change.
f) Despite the uniform m_c observed along the depth of MICP-treated columns, the morphology of the $CaCO_3$ cemented between the sand particles after MICP treatment gradually changes, which influence the strength change of treated sand.

The study finds that the key factors affecting the localized compressive strength of MICP-treated sand columns are the localized water content and morphological changes in the $CaCO_3$ cementation taking place locally over time along the column depth. This work does not analyze the influencing factors such as specimen scale and particle size distribution which should be addressed in the future works. Also, the results presented in this study must also be analyzed after upscaling the specimen. Additionally, an analysis of the implications of these findings in field applications using the surface percolation method would provide important insights.

Acknowledgments

This work was supported by the Basic Science Research Program through the National Research Foundation of Korea funded by the Ministry of Education (2021R1I1A3049493).

References

Ashraf, M.S., Azahar, S.B. and Yusof, N.Z. (2017), "Soil improvement using MICP and biopolymers: A revie.", *IOP Conference Series: Materials Science and Engineering*, **226**(1), 12058. https://doi.org/10.1088/1757-899X/226/1/012058.

Cheng, L. and Cord-Ruwisch, R. (2012), "In situ soil cementation with ureolytic bacteria by surface percolation", *Ecol. Eng.*, **42**, 64-72. https://doi.org/10.1016/j.ecoleng.2012.01.013.

Cheng, L. and Cord-Ruwisch, R. (2014), "Upscaling effects of soil improvement by microbially induced calcite precipitation by surface percolation", *Geomicrobiol. J.*, **31**(5), 396-406. https://doi.org/10.1080/01490451.2013.836579.

Cheng, L. and Shahin, M.A. (2019), "Microbially Induced Calcite Precipitation (MICP) for soil stabilization", *Ecol. Wisdom Inspired Restoration Eng.*, 47-68. Springer. https://doi.org/10.1007/978-981-13-0149-0_3.

Cheng, L., Shahin, M.A., Cord-Ruwisch, R., Addis, M., Hartanto, T. and Elms, C. (2014), "Soil stabilisation by microbial-induced calcite precipitation (MICP): investigation into some physical and environmental aspects", *Proceedings of the 7th International Congress on Environmental Geotechnics*, Engineers Australia Melbourne, Australia.

Choi, S.G., Chang, I., Lee, M., Lee, J.H., Han, J.T. and Kwon, T.H. (2020), "Review on geotechnical engineering properties of sands treated by microbially induced calcium carbonate precipitation (MICP) and biopolymers", *Constr. Build. Mater.*, **246**, 118415. https://doi.org/10.1016/j.conbuildmat.2020.118415.

DeJong, J.T., Mortensen, B.M., Martinez, B.C. and Nelson, D.C. (2010), "Bio-mediated soil improvement.", *Ecol. Eng.*, **36**(2), 197-210. https://doi.org/10.1016/j.ecoleng.2008.12.029.

Do, J., Montoya, B.M..and Gabr, M.A. (2019), "Debonding of microbially induced carbonate precipitation-stabilized sand by shearing and erosion", *Geomech. Eng.*, **17**(5), 429-438. https://doi.org/10.12989/gae.2019.17.5.429.

Fouladi, A.S., Arulrajah, A., Chu, J., Zhou, A. and Horpibulsuk, S. (2024), "Factors affecting the MICP stabilization of washed recycled sands derived from demolition wastes", *Acta Geotechnica*, 1-22, https://doi.org/10.1007/s11440-024-02396-8.

Gowthaman, S., Iki, T., Nakashima, K., Ebina, K. and Kawasaki, S. (2019), "Feasibility study for slope soil stabilization by microbial induced carbonate precipitation (MICP) using indigenous bacteria isolated from cold subarctic region", *SN Appl. Sci.*, **1**, 1-16. https://doi.org/10.1007/s42452-019-1508-y.

Ivanov, V., Stabnikov, V. and Kawasaki, S. (2019), "Ecofriendly calcium phosphate and calcium bicarbonate biogrouts", *J. Cleaner Product.*, **218**, 328-334. https://doi.org/10.1016/j.jclepro.2019.01.315.

Kalkan, E. (2020), "A review on the microbial induced carbonate precipitation MICP for soil stabilization", *Int. J. Earth Sci. Knowledge Appl.*, **2**(1), 38-47. https://dergipark.org.tr/en/pub/ijeska/issue/55459/760031.

Konstantinou, C., Wang, Y., Biscontin, G. and Soga, K. (2021), "The role of bacterial urease activity on the uniformity of carbonate precipitation profiles of bio-treated coarse sand specimens", *Scientific Reports*, **11**(1), 6161. https://doi.org/10.1038/s41598-021-85712-6.

Li, S., Huang, M., Cui, M., Lin, P., Xu, L. and Xu, K. (2023), "Stabilization of cement-soil utilizing microbially induced carbonate precipitation", *Geomech. Eng.*, **35**(1), 95-108. https://doi.org/10.12989/gae.2023.35.1.095.

Lv, C., Zhu, C., Tang, C.S., Cheng, Q., Yin, L.Y. and Shi, B. (2021), "Effect of fiber reinforcement on the mechanical behavior of bio-cemented sand", *Geosynth. Int.*, **28**(2), 195-205. https://doi.org/10.1680/jgein.20.00037.

Mahawish, A., Bouazza, A. and Gates, W.P. (2019), "Unconfined compressive strength and visualization of the microstructure of coarse sand subjected to different biocementation levels", *J. Geotech. Geoenviron. Eng.*, **145**(8), 04019033. https://doi.org/10.1061/(ASCE)GT.1943-5606.0002066.

Maleki Kakelar, M., Yavari, M., Yousefi, M.R. and Nimtaj, A. (2020), "The influential factors in the effectiveness of microbial

induced carbonate precipitation (MICP) for soil consolidation", *J. Human Environ. Health Promot.*, **6**(1), 40-46. http://dx.doi.org/10.29252/jhehp.6.1.8.

Nawarathna, T.H.K., Gowthaman, S., Nakashima, K. and Kawasaki, S. (2022), "Organic-Inorganic Hybrid Green Materials for Soil Improvement", *Encyclopedia of Green Mater.*, 1-10. Springer. https://doi.org/10.1007/978-981-16-4921-9_274-1.

O'Donnell, S.T., Kavazanjian Jr., E. and Rittmann, B.E. (2017), "MIDP: Liquefaction mitigation via microbial denitrification as a two-stage process. II: MICP", *J. Geotech. Geoenviron. Eng.*, **143**(12), 4017095. https://doi.org/10.1061/(ASCE)GT.1943-5606.0001818.

Pratama, G.B.S., Yasuhara, H., Kinoshita, N., Putra, A., Almajed, A., Fukugaichi, S. and Ihsani, Z.M. (2024), "Efficacy of soybean-derived crude extract in enzyme-induced carbonate precipitation as soil-improvement technique", *Int. J. Geo-Eng.*, **15**(1), 14. https://doi.org/10.1186/s40703-024-00204-6.

Shahrokhi-Shahraki, R., Zomorodian, S.M.A., Niazi, A. and O'Kelly, B.C. (2015), "Improving sand with microbial-induced carbonate precipitation", *Proceedings of the Institution of Civil Engineers-Ground Improvement*, **168**(3), 217-230. https://doi.org/10.1680/grim.14.00001.

Sierra, K., An, J., Shamet, R., Chen, J., Kim, Y.J., Nam, B.H. and Park, P. (2024), "A review of geopolymer binder as a grouting material.", *Int. J. Geo-Eng.*, **15**(1), 21. https://doi.org/10.1186/s40703-024-00221-5.

Wang, H.L. andYin, Z.Y. (2021), "Unconfined compressive strength of bio-cemented sand: state-of-the-art review and MEP-MC-based model development", *J. Cleaner Product.*, **315**, 128205. https://doi.org/10.1016/j.jclepro.2021.128205.

Wang, Y., Jiang, R., Wang, G. and Jiao, M. (2023), "Study on mechanical properties of Yellow River silt solidified by MICP technology", *Geomech. Eng.*, **32**(3), 347-359. https://doi.org/10.12989/gae.2023.32.3.347.

Wang, Y., Wang, G., Wan, Y., Yu, X., Zhao, J. and Shao, J. (2022), "Recycling of dredged river silt reinforced by an eco-friendly technology as microbial induced calcium carbonate precipitation (MICP)", *Soils Found.*, **62**(6), 101216. https://doi.org/10.1016/j.sandf.2022.101216.

Xiao, Y., He, X., Evans, T.M., Stuedlein, A.W. and Liu, H. (2019), "Unconfined compressive and splitting tensile strength of basalt fiber–reinforced biocemented sand", *J. Geotech. Geoenviron. Eng.*, **145**(9), 04019048. https://doi.org/10.1061/(ASCE)GT.1943-5606.0002108.